



## Synthesis, Characterization and study the Optical properties of Ag/ TiO<sub>2</sub> nanoparticles and its Biological Application

**Nada Abdul Hadi Kareem**

**University of Al-Qadisiyah/ College of Education/ Department of Physics**

**E:mail: nada.almislimawy@qu.edu.iq**

### Abstract

Ag and TiO<sub>2</sub> nanoparticles and hybrid Ag/TiO<sub>2</sub> nano particles were synthesized using nanosecond pulsed laser method. The effect of the number of the pulses (450) on the structural, optical characteristics of nanoparticles destined in distilled water DW as growth media was tested by a Q- Switched Nd-YAG laser wavelength of (1064) nm., The ablation energy of 530 mJ with repetition rate of 1 HZ . The prepared nanoparticles and hybrid nanoparticles were characterized using (UV\_Vis) spectroscopy, (XRD), (FESEM) and (EDX). The functional groups of (TiO<sub>2</sub>/Ag) in liquid media were discovered using the FTIR method. Almost spherical nano- and microparticles are seen in TEM images used for optical diagnostics. The (284.1) and (418.3) nm wavelengths, which are virtually equal to the absorption spectra of a solution containing nanoparticles. The prepared nanoparticles (Ag, TiO<sub>2</sub>) and hybrid nanoparticles (AgTiO<sub>2</sub>: 1:1, 1:2, 1:3 ) were investigated for their biological application. The UV-Vis spectrum for pure silver nanoparticles display a slightly broad absorbance peak in the range 384 - 410 nm which is diagnostic of surface plasmon resonance for (Ag) nanoparticles. The effects of Laser Shots on Absorbency and Surface Plasmon Resonance were studied, the colour of nano solution changed from light to dark with the number of laser pulses increased. This indicates the formation of a solution containing metal nanoparticles in distilled water. The synthesized material exhibited promising activity against the bacterial pathogens such as Escherichia coli and Staphylococcus aureus.

Key word: Hybrid Ag and TiO<sub>2</sub> , laser ablation ,nanoparticles , biological application.

## **1: Introduction:**

Due to ongoing efforts to synthesize nanoparticles and other objects smaller than a nanometer using a variety of tools and processes, nanoscience has appeared as a notable research area in our recent society [1]. According to their size and shape, metal nanoparticles have superior plasmon resonance characteristics [2]. Because of their exceeding magnetic, electrical, and optical properties, colloidal metal nanoparticles are of essential benefit to investigators in a mixture of domains, include materials science, physics, engineering, and chemistry [3-4]. Metallic nanoparticles' power to trap electrons at the nanoscale is what supply them their surface plasmon resonance (SPR) characteristic. Conditional their size and shape, metal nanoparticles have fantastic characteristic include plasmon resonance belongings [5]. How to make nanostructures with a made-to-order shape that works for different applications and from different materials is a important situation in the field of nanotechnology. The two primary kind of nanostructure fiction method are bottom-up assembly and top-down composition [6]. Since the 1960s, when the ruby laser was investigated, top-down laser ablation of materials has been utilized [7-8]. The nucleation, development, and cluster fabrication of laser-ablated species are mostly a bottom-up process for creating nanoparticles using laser ablation [9].

In current study, colloidal solutions of titanium dioxide and silver were prepared. The results of the effects of some laser treatments on the properties of the prepared nanoparticles as well as the outcome of examination of XRD size and shape of the nanoparticles are discussed by means of field emission scanning electron microscopy (FE-SEM), (TEM), absorption spectroscopy (UV-Vis), FTIR absorption measurement, the effects of Laser Shots on Absorbency and Surface Plasmon Resonance were studied, and the effect of these nanoscale solutions on biological application on two types of bacteria were studied also.

## **2: Methods and Materials:**

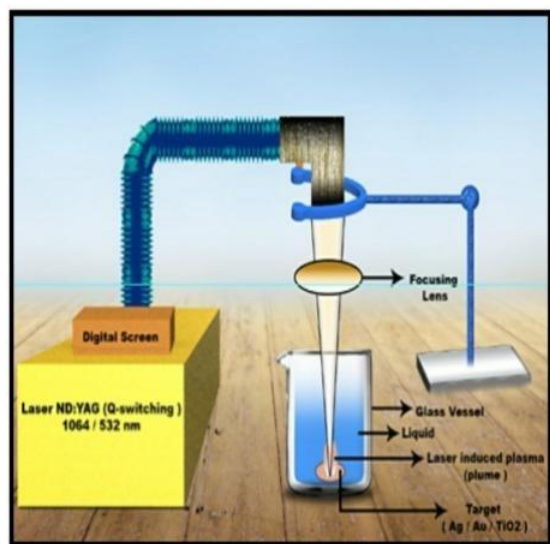
Amorphous, polycrystalline, and single-crystal particles are among the NPs. A material is considered to have no dimensions when all of its dimensions are measured at the nanoscale. Amorphous, single-crystal, and polycrystalline particles make up these nanoparticles (NPs). They can also be referred to as NPs in any shape, such as cubes, spheres, or platelets. "Nanocrystals" is

the term used to describe NPs that are single crystals. When NPs have tiny enough dimensions and exhibit quantum confinement effects, the name "quantum dots" is commonly applied to them [10]. Secondly, one dimension that is not tiny is present in one-dimensional nanomaterials, or 1-D nanomaterials. This kind has also been referred to as nanowires, nanorods, filaments, and fibers. In one-dimensional systems, carbon, metal, or even oxide-based systems are usually considered. If one-dimensional extension predominates over other species, then one-dimensional structures can also be conceived of as nanotubes and nanocables. [10–11]. Third - Two-dimensional materials and two-dimensional nanostructures are examples of two-dimensional substances that are not limited to the nanoscale. Nanostructures have been the focus of extensive research for over a century due to their greater significance and variety of forms, including nanofilms, nanolayers, nanocoatings, and nanodiscs [12–13]. Fourth: Bulk nanomaterials, sometimes referred to as three-dimensional nanomaterials, are challenging to categorize. Conversely, materials that are not restricted to the nanoscale might be referred to as bulk nanomaterials. These materials are distinguished above 100 nm by their three randomly distributed dimensions [14].

Titanium dioxide (TiO<sub>2</sub>) colloidal nanocrystalline solutions have been prepared using both the non-noble metal titanium and the noble metal silver (Ag). Following the production of the hybrid material, supplies and instruments required to analyze the structural and optical characteristics of the nanoparticles were prepared using laser ablation pulses.

With an effective beam width of (2) mm for metallic targets have a high purity of 9.99%, the device has a Q-Switched Nd: YAG laser source with two wavelengths (1064 and 532) nm, a maximum energy of (1000 mJ per pulse), pulse duration of (10 ns), repetition frequency of (6 Hz), also other characteristic. (Titanium and Silver). A 20 cm focal length lens was employed to provide a strong laser flux.

Colloidal solutions of metallic nanoparticles were prepared by using high purity (9.99%) titanium and silver targets using pulsed laser ablation laser (PLAL) technology. according to the figure. (1) The metal targets were cleaned also polished by ethanol wash both before to and after each resection stage. distilled water (DW) in a glass vial, with a fluid height of four millimeters above the target surface and a volume of five milliliters utilized in all ablation processes. After that, the targets were cleansed with water using an ultrasound system (ultrasound route) to get rid of any remaining pollutants.



**Figure(1) shows the experimental set up of the nanosecond pulsed laser method**

According to the most current investigation, the No. of laser pulses was influenced by the intensities of the individual laser pulses. The energy consumed by each pulse is (530) mJ. A constant (530) megajoule laser energy is applied to the target metal surface in the form of (450) laser pulses. The laser beam's surface diameter for each metal target utilized in this investigation was (2) mm, and precise measurement was made possible by the (8) cm space between the target and the laser lens. To create colored colloidal solutions include nanoparticles for the metallic targets, the targets were exposed to a (Nd:YAG) laser with a (1064 nm) wavelength, a (10) nm pulse period, and a (1 Hz) frequency. which, as part of the eradication procedure, was later removed when the color of the water changed. TEM it's a method used to exam objects with electrons. Surface plasmon resonance and absorbance were measured using a wave number (FTIR) device (TEM), and structural and surface features were evaluated using an X-ray diffractometer. Additionally, optical properties were studied in relation to the impact of laser shoots on absorbency and surface plasmon resonance.

### 3: Results and Discussion:

#### 3-1 Structural and Morphological properties of Nanoparticles

the examination of the physical characteristics of the structures made of nanoparticles using the pulse laser ablation (PLAL) technique. The X-ray diffraction pattern (XRD) was used to establish the crystal's size, and the FE-SEM and TEM examinations were used to assess the size and form of the particle samples.

##### 3-1-2 X-Ray Diffraction Results

X-ray diffraction patterns were examined for all the prepared samples, which were ( 530 mJ ), and (450) pules to measure the crystal size by determining the Full width of half maximum , Miller's coefficients, the peak position and calculating the crystal size by applying the Scherer equation, where the results were as follows : -

##### 3-1-3 XRD of Ag Nanoparticles:

In this study the crystal system is polycrystalline and have cubic shape, as a results of the XRD of the Ag nanoparticles deposited on the glass substrate. Figure (2) exhibit the peaks at the angles (38.40, 44.64, 64.84, 77.88), that match to the planes (111, 200, 220, 311). Additionally, the obtained results demonstrated that the shape (2) and the dominant direction (111) of the crystal plane are consistent with the researcher's findings [15] and [16], and that the spacing between the atomic levels (d) and the diffraction angle ( $2\theta$ ) match to all diffraction peaks are identical with the standard data (JCPDSCard No.04-0783) of Ag material.

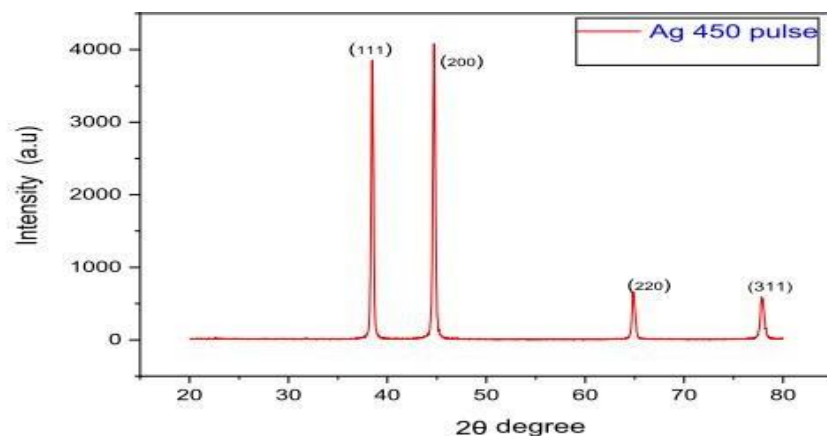


Figure (2) illustrates XRD pattern of Ag Nanoparticles.

### 3-1-4 -2 X-Ray Diffraction Of Titanium Dioxide Nanoparticles

The titanium dioxide nanoparticle solution was deposited on a glass slide, as depicted in figure (3). The XRD pattern for the nanoparticles revealed the emergence of a quadrangular crystal system, and it was determined that the particles are in the (Rutile) phase. We also noticed that the angles (27.6, 36.2, 41.45, 54.45) correspond to the planes (110, 101, 111, 211).

All of the diffraction peaks in this set of data roughly correlate to the conventional titanium dioxide pattern (JCPDS Card No. 04-0783). The crystal plane is oriented dominantly toward (110).

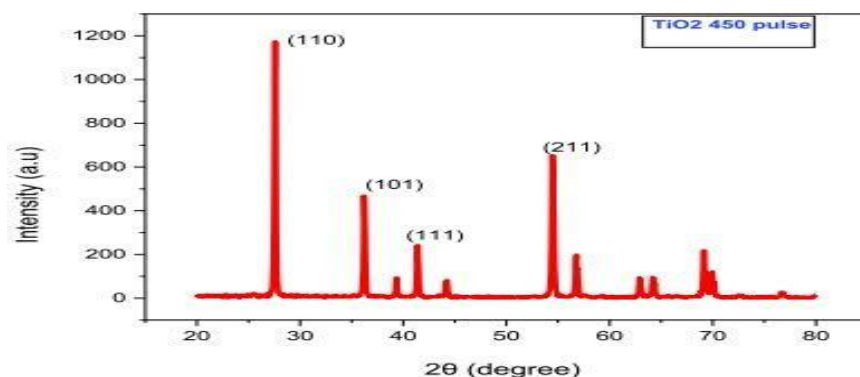


Figure (3) illustrates XRD pattern of the TiO<sub>2</sub> nanoparticles.

As shown in Table (1) the results of the experiments as comparing with the standard results for international labels for each of the titanium dioxide and silver nanoparticles for each of them with their respective levels.

Table (1) shows the results of XRD for each of the TiO<sub>2</sub> and Ag nanoparticles

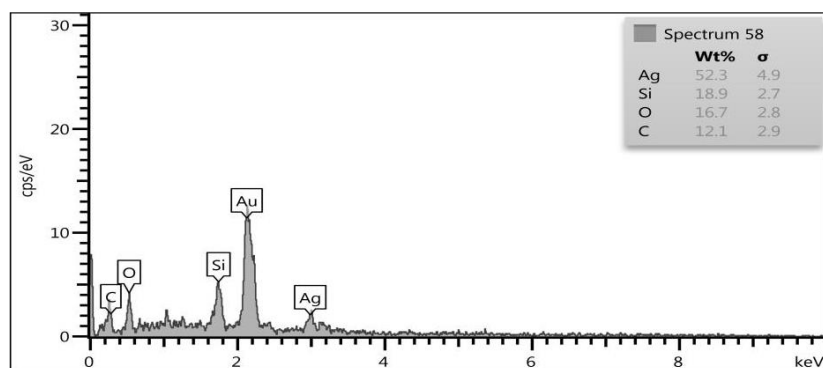
Nanomaterial	2θ (deg) Experimental	2θ (deg) Standard	FWHM (deg)	D (nm) Crystal size	d <sub>hkl</sub> (nm) Experimental	d <sub>hkl</sub> (nm) Standard	hkl
Ag	38.40	38.116	0.2721 5	30.93258 65	0.2337540 3	0.235902 21	11 1
	44.64	44.277	0.3028 5	28.37808 09	0.2024789	0.204401 39	22 2
	64.84	64.426	0.0919 3	102.3989 66	0.1437554 1	0.144499 32	22 0
	77.88	77.472	0.4790 8	21.33575 43	0.1225043 5	0.123100 45	31 1
TiO <sub>2</sub>	27.6	27.446	0.2280 5	39.34223 69	0.1660391 8	0.167120 69	11 0
	36.2	36.085	0.2031 2	48.50937 07	0.1303288 3	0.130780 96	10 1
	41.4	41.225	0.2109 4	50.23188 41	0.1164775 7	0.116883 05	11 1
	54.45	54.322	0.2645 6	51.72250 13	0.0946273 5	0.094826 16	21 1

### 3-2-1 The Field Emission Scanning Electron Microscopy (FESEM) Results

FESEM assay was performed for all samples obtained by laser ablation method in distilled water to study surface topography that photographed the surface at high magnification. It is obtained with (450)pulses and constant energy . The size ratios of these particles were calculated by the software (image j) . These photos of the various-sized nanoparticles on the substrates show the shape dispersion. FE-SEM images and titanium dioxide and silver nanoparticle size distributions calculated with Origin Pro 8.5 software are displayed in Figures (4), (6), and (8).

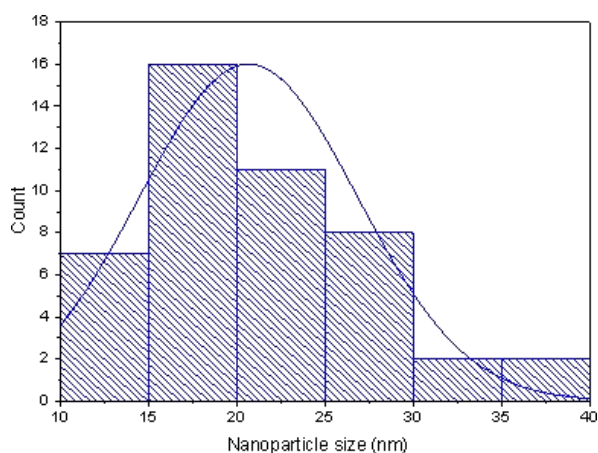
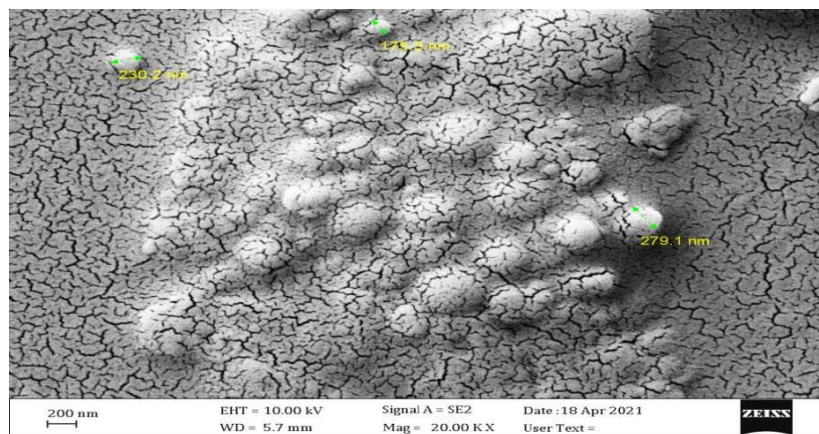


The EDX diagram in Figure (5) display the sample (AgNPS) which produced by (450 pulses) and an ablation energy of(530 mJ) in a distilled water, where the presence of(Ag) (O),(C),(Si) elements was obtained. The environment around the device (EDX) contains certain components, and as a result of the internal surface of the device being coated using gold metal, the largest peak of gold (Au) emerges. The material was coated with materials with great conductivity and small granular sizes to create a pleasant image. This increases the signal-to-noise ratio and reduces noise during shooting.



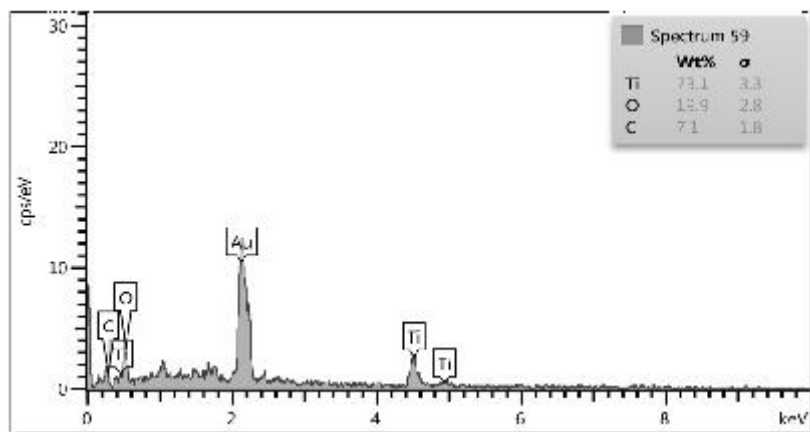
**Figure (5): EDX chart of the Ag Nanoparticles .**

Figure (6) shows (FE-SEM) images of titanium dioxide nanoparticles with (450) pulses, (530) mJ energy pules laser, and the diagonal distribution of the particles. We note from chart that particles were obtained within the nanoscale ranged between (10.0 – 36.346 ) nm with average size of diameters (20.583 nm) and almost spherical.



**Figure (6) FE-SEM image of a Titanium Dioxide Nanoparticle and Histogram and Kaosi diagram.**

The ( $\text{TiO}_2$  nanoparticles) sample formed using (450) pulses and the energy of ablation (530 mJ) in distilled water medium are illustrated in Figure (7) along with the EDX scheme, where we found the existence of (Ti, O, C) elements. However we see the emergence of the greatest peak of gold (Au) for the surface of the EDX sample, whose inner surface is covered with a golden metal, some of the elements that were obtained due to the environment around the (EDX) sample include these elements.



**Figure (7) EDX chart of TiO<sub>2</sub> Nanoparticle.**

Field Emission Scanning Electron Microscopy pictures of hybrid nanoparticles of titanium dioxide/silver at 450 pulses, 530 mJ of energy, and particle diameter distribution are displayed in Figure (8). We can noticed that the particles were practically spherical, and the average diameter equal to (84.992 nm), and that they were produced within the nanoscale range of (45.714 – 182.946 nm).

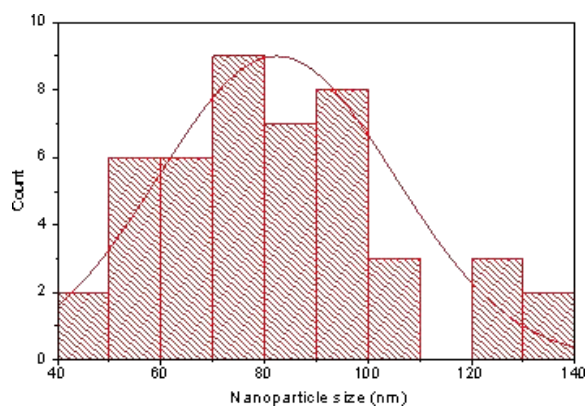
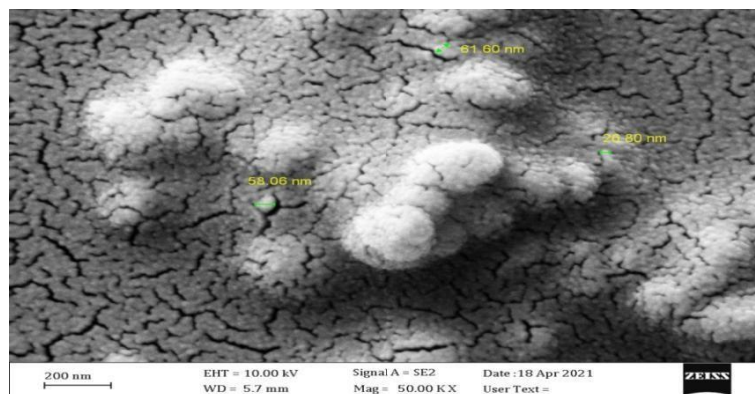


**Figure (8) FE-SEM image of Hybrid Nanoparticles of Titanium Dioxide / Silver and Diagram and Kaosi diagram .**

The hybrid titanium dioxide/silver nanoparticles generated with (450 pulses) and the energy of ablation was (530 mJ) in distilled water medium are shown in Figure (9) along with the EDX scheme, where we noticed the presence of (Ti, Ag, O, C) components. However we see the emergence of the maximum peak of (Au gold) owing to the surface of the (EDX) sample, whose inner surface is covered with a golden metal, some of the elements that were obtained due to the environment around the (EDX) sample include these elements.

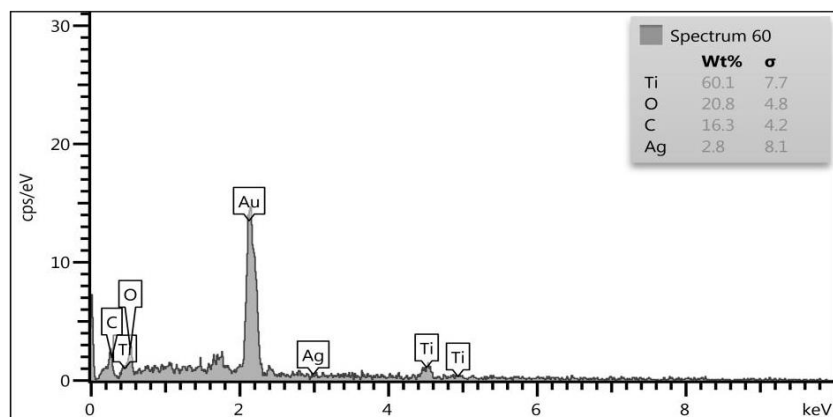


**Figure (9) EDX Diagram of the Hybrid (TiO<sub>2</sub> / Ag) Nanoparticles.**

### 3-2-2 Transmission Electron Microscopy (TEM) analyses

The majority of the metal nanoparticles were spherical, as seen by the TEM picture. DW (Distilled water) was used to create mineral colloidal solutions at a wavelength of (1064 nm) of the Nd: Yag laser, 450 pulses per pulse, and 530 mJ of energy. Figure (10) displays (TEM) images that were measured at two different scales (50 and 100 nm). The statistical distribution of the particle diameters of the colloidal solution of the (Ag) nanoparticles was shown in image of Figure (10), which is apparent where the diameters of the particles are approximately accumulated at 17 and 8 nm, respectively, for the scales. It was discovered that the NPs were almost there appearance was spherical, and the distribution of some particles and their shape at a large size was caused by the clustering phenomenon [18], as incontestable using (TEM) images were tested at various scales and accompanying the statistical distribution that were planned in (Origin pro 8.5).

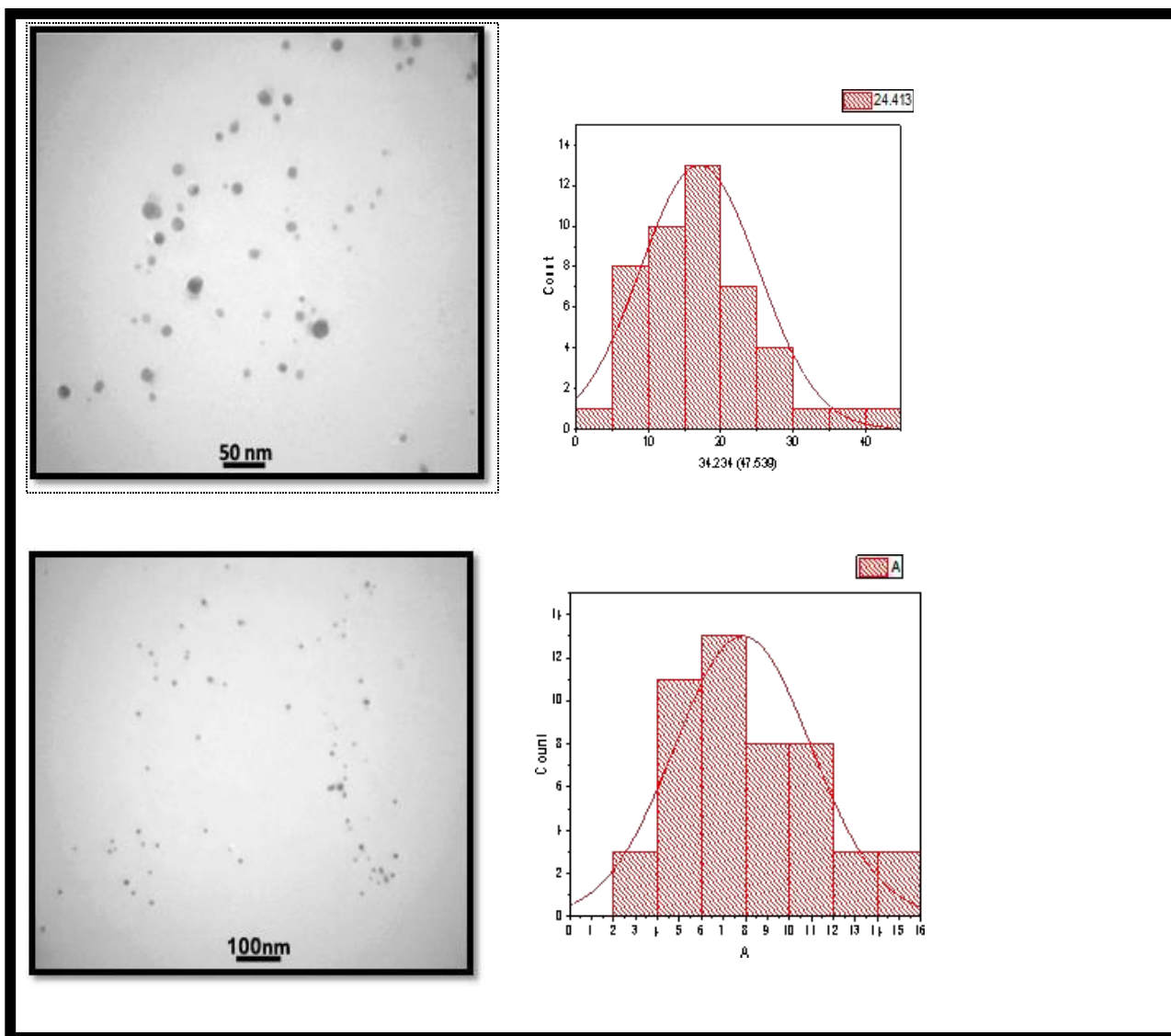


**Figure (10) illustrates colloidal solution of the produced Ag NPs along with the particle size distribution and TEM images.**

Figure(11) shows the TiO<sub>2</sub> NPs solution and the distribution of the diameters of these particles at various scales 50, 100 nanometers are shown in (TEM) pictures in Figure 11. For varying scales, the graph displays the approximate location of the diagonals' distribution centers at (58 and 25) nm.

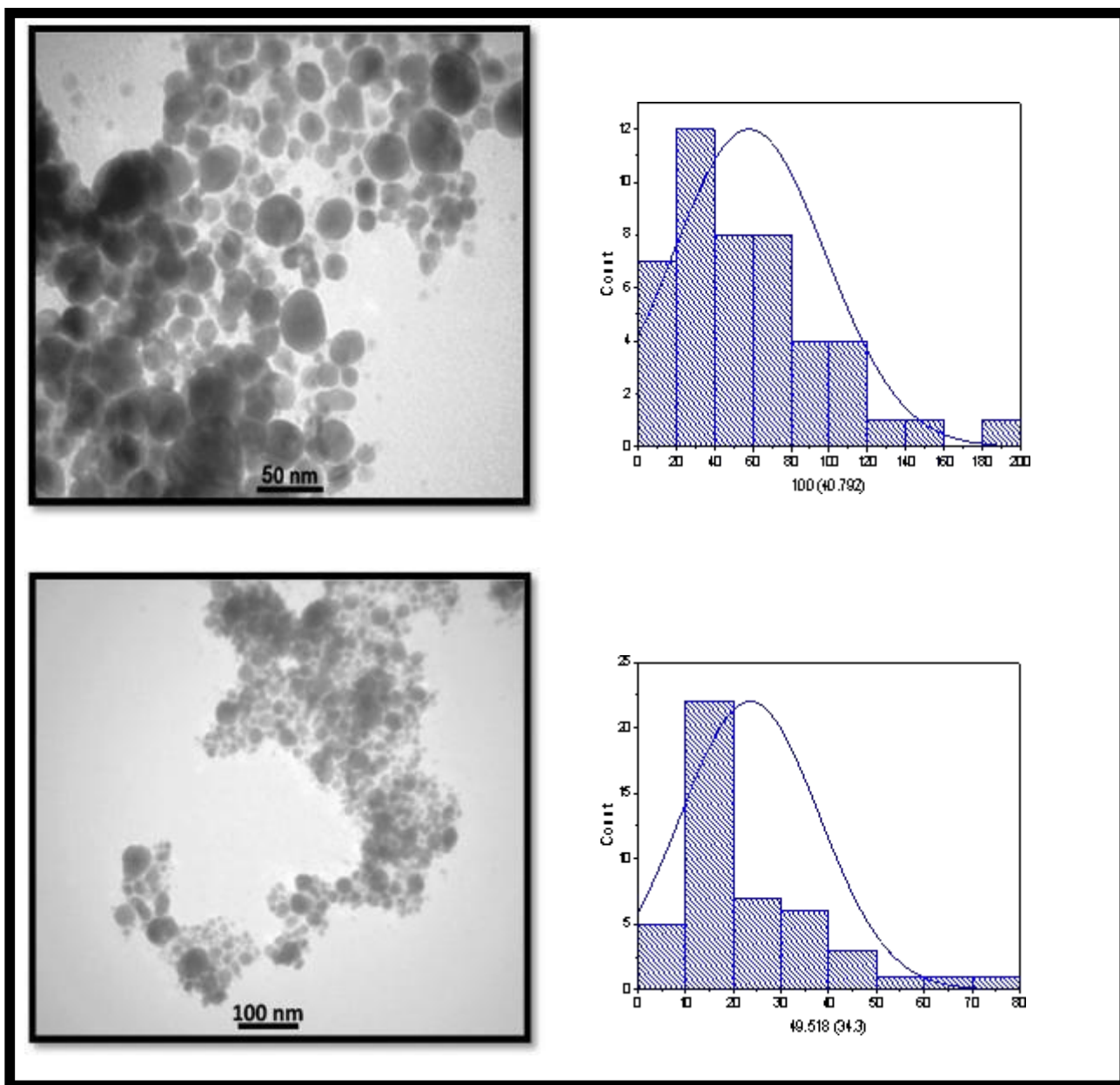
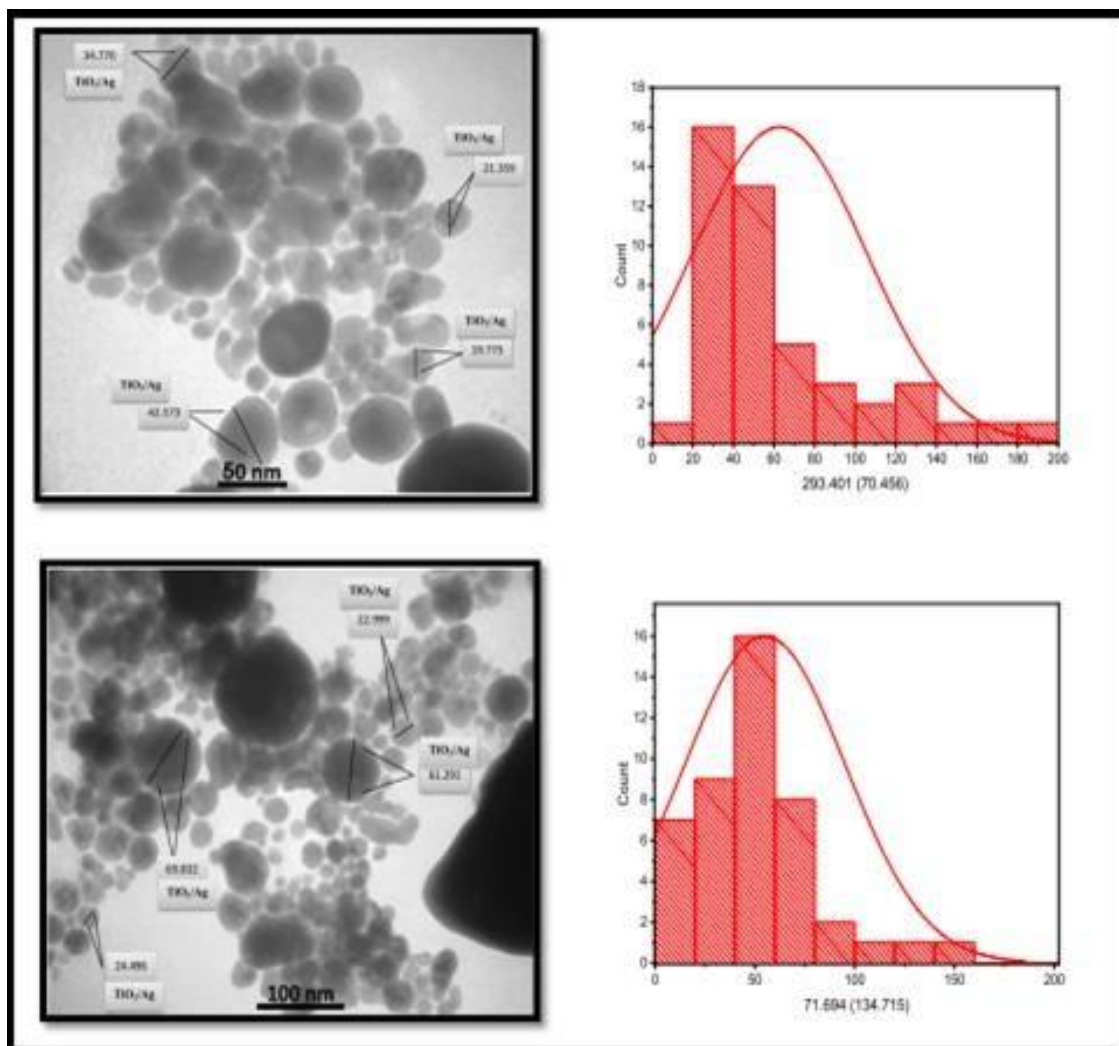


Figure (11) shows  $\text{TiO}_2$  in a colloidal solution: TEM images and particle size distribution ).

In the figure above its clear that the distribution of the diameters of the hybrid  $\text{TiO}_2/\text{Ag}$  NPs at various scales (50 and 100 nm) is depicted in Figure (12) along with transmission electron microscopy (TEM) pictures of the solution. The diagonal distribution's approximate centering at (65 and 60) nm is depicted on the graph.



**Figure (12) TEM pictures and the colloidal solution's particle size distribution for hybrid titanium dioxide/silver nanoparticles are shown above**

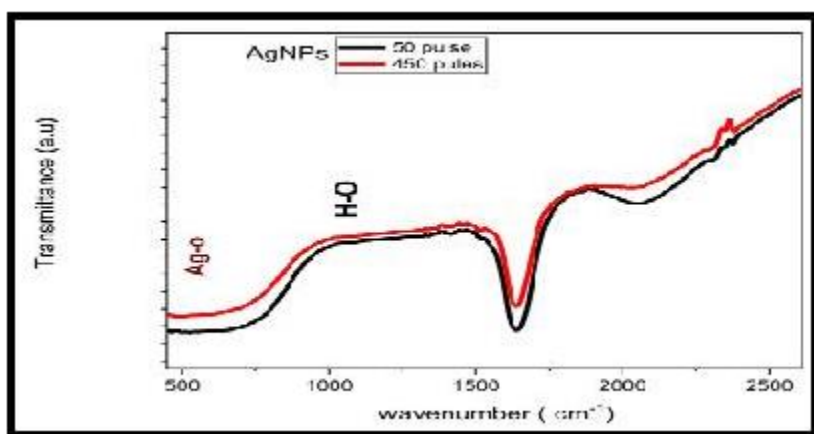
### 3-2-3 FTIR test results:

In this study infrared spectroscopy is a significant laboratory test that provides important content about the location of ions in the crystal structure by analyzing oscillation [19-20].

The measurement was conducted to determine the biomolecules accountable for detecting, reducing the factor of the NPs that were removed by the (PLAL). Infrared spectroscopy (FTIR)

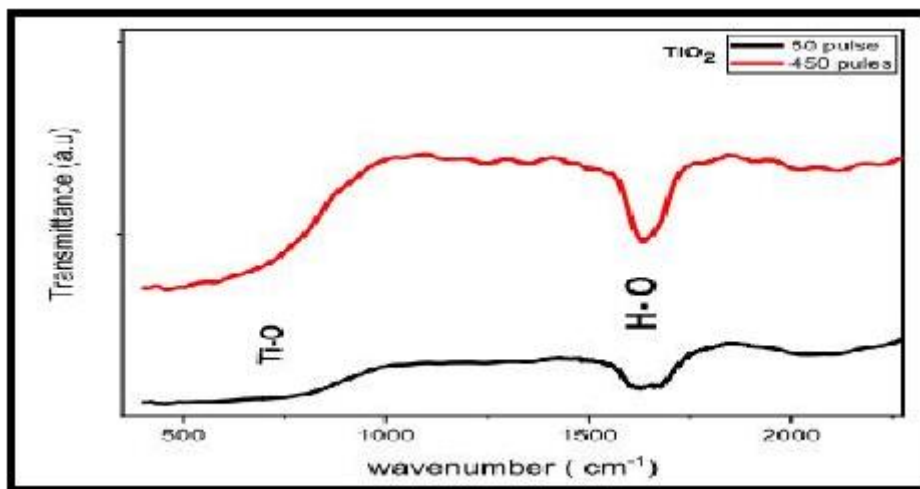
was used to determine the active groups (chemical bonds) and identify the compound based on its characteristics. Each compound exhibits its own absorbance due to the absorption of chemical bonds within the range of (400-4000)  $\text{cm}^{-1}$ . On the other hand the infrared spectroscopy analysis of the solution include Ag NPs and  $\text{TiO}_2$  discovered the existence of several clusters, indicating the presence of many active groups inside these particles [21].

Figure (13) displays the IR spectrum of silver nanoparticles processed in (DW) using (50,450 pulses) while the ablation energy was constant at (530 mJ). The spectrum reveals the existence of distinct functional groups in the pure AgNPs. Notably, the absorption bond at a wave number of  $468.77 \text{ cm}^{-1}$  corresponds to the vibration of the Ag-O bond, while the absorption bond at a wave number of  $1641 \text{ cm}^{-1}$  agree with the vibration of the H-O group [22].



**Figure (13) (FTIR spectra) of a solution of silver Nanoparticles**

In figure14 (FTIR spectroscopy) sites and connections of chemical compounds and bond sites for titanium dioxide nanoparticles were prepared in (DW) medium with pulse numbers of (50-450 pulses) at a constant ablation energy of (530 mJ). It is cleared that the absorption beam near the wave number of ( $478.3463 \text{ cm}^{-1}$ ) is caused by the vibration of the Ti-O coupling, while the absorption beam near the wave number of ( $1660.71 \text{ cm}^{-1}$ ) is caused by the vibration of the H-O functional group [22-23].



**Figure (14) FTIR transforms of the infrared spectra of a solution containing TiO<sub>2</sub>NPs**

Figure (15) displays the locations of FTIR sites, the linkages between chemical compounds, and the sites of bonds for hybrid particles consisting of titanium dioxide and silver. The absorption peak seen at wave numbers (443.77, 484.13 cm<sup>-1</sup>) is a result of the coupling vibration between the (Ti-O) and (Ag-O) bonds. Similarly, the absorption peak observed at wave number (1635.635 cm<sup>-1</sup>) is attributed to the vibration of the (H-O) group in the sample [22, 23].

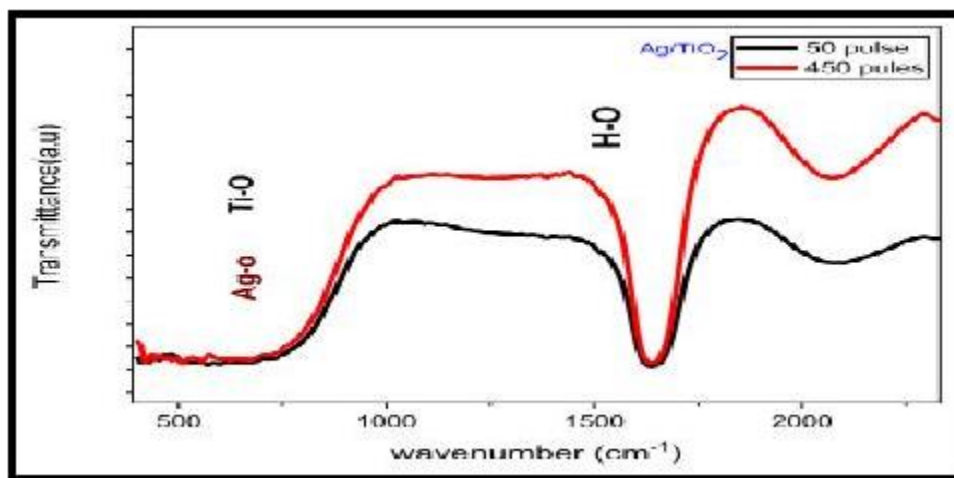


**Figure (15) illustrates the Fourier transforms of the infrared spectrum of a solution of hybrid TiO<sub>2</sub>/Ag**

### 3-4 Optical Properties

In order to study the impact of laser pulses on the characteristics and size of nanoparticles at energy (530 mJ) and the number of different pulses (50, 250, 450), colloidal solutions containing nanoparticles of target metals titanium dioxide and silver were created using the pulsed laser ablation in liquid (PLAL) technique. It was discovered that the color of the solution changed and its intensity increased when the number of laser pulses increased. This indicates the formation of a solution containing metal nanopa in distilled water and using the wavelength of the laser used (1064 nm). This modification results from the oscillation and cohesion of electrons on the nanoparticle surfaces, an increase in the quantity and size of excised particles, and an increase in the absorbance intensity with the number of pulses [24]. By using the optical and ultraviolet ray spectroscopy data for the colloidal solutions made for silver, titanium dioxide, and hybrid, respectively, as shown in Figures (16), (17), and (18). The results of the SPR spectrum and the absorbance intensity calculated from the absorbance spectrum are shown in Table (2). Since the increase in laser pulses caused an increase in the absorbance intensity and an increase in the intensity of the SPR peaks, the changes were found to be within the visible spectrum of silver and the ultraviolet region of titanium dioxide solution, according to an analysis of the absorption spectrum. The amount of laser pulses had an impact on the absorption peaks' width and height. The spectral change suggests that laser irradiation increased the abundance of nanoparticles, and we noticed the presence of a plasmon peak, which indicates that the nanoparticles were almost spherical in shape [25, 26].

The absorption spectrum of the silver nanoparticle solution is depicted in Figure (16), and the location of the plasmon peak at around (412 nm), as shown in Table (2), suggests that the shape of the nanoparticles is nearly spherical [27].

The created samples' findings for the absorption spectra of the silver nanoscale solution revealed (50, 250, and 450) pulses. The characteristics of the resultant nanoparticles can be significantly impacted by the bubble mechanism and the high energy associated with bubble collapse [28]. By scattering the laser pulses, the bubbles can lower the method's yield [29]. When the bubble pops, the nanoparticles are released into the liquid, where they continue to grow for a short time through condensation of the excised atoms. The smaller particles are incorporated into the larger

particles, and as the number of pulses rises, so does the particle size [30]. The outcomes of (FE-SEM) and (TEM) spectroscopies are proof that metal nanoparticles form in solution.

Figure (17) displays the peaks of Surface Plasmon Resonance (SPR) for a colloidal solution containing titanium dioxide nanoparticles. With an increase in the number of pulses, a greater quantity of nanoparticles was generated. These nanoparticles exhibited a significant absorption capacity at shorter wavelengths in the UV spectrum, resulting in an overall increase in optical absorption [31]. The investigation determined that the surface plasmon resonance peaks of the titanium dioxide particles were located at 291, 293, and 292 nm in the produced samples. The particles that are eliminated and discharged from the target are shown in table (2) as still present in the liquid around the target, leading to the formation of a colloidal solution. These particles possess the capacity to assimilate laser energy, resulting in a reduction of the laser's light output. Three aspects that are expected to influence the success of eradicating the targets are: altering the polarity of the solution, enhancing diffusion through a high concentration of nanoparticles, and surface imperfections [32].

The existence of nanoparticles might lead to a change in the color of the solution, depending on the extent of nanoparticle aggregation [33].

According to Table (2), the hybrid nanoparticles' surface plasmon resonance peaks were fixed in place, and Figure (18) shows the absorption spectra of the silver and titanium dioxide nanoparticle solution. For each, we see that there are two plasmon peak places. Almost (291) nm at the starting point. The hybrid nanoparticles' second location's peak positions, which we also noticed, were (from 413-417, 408-413, and 415-419) nm.

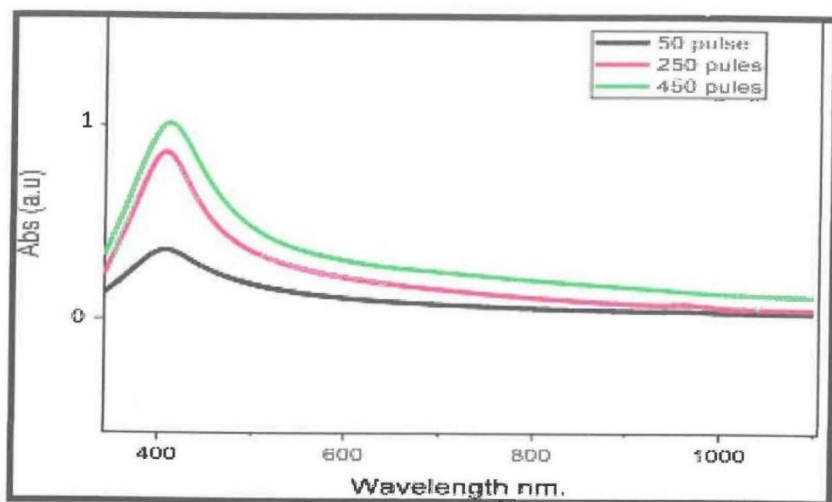


Figure (16) The absorbance of silver nanoparticles solution.

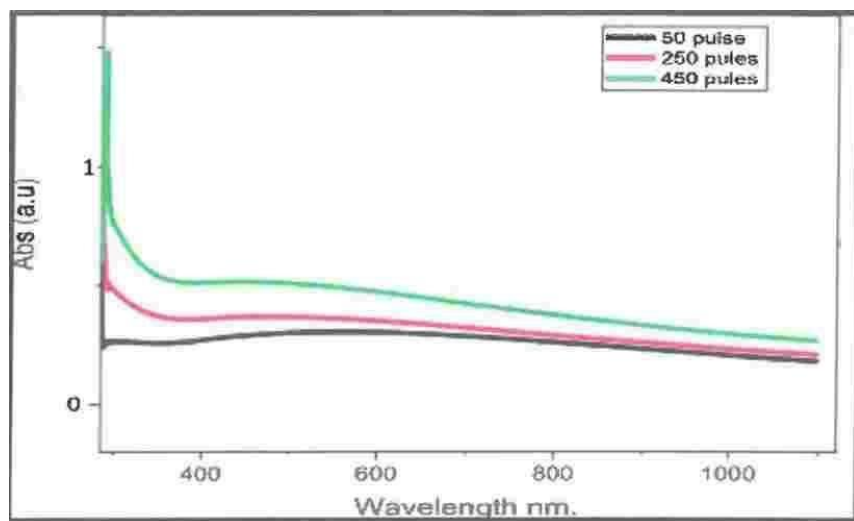
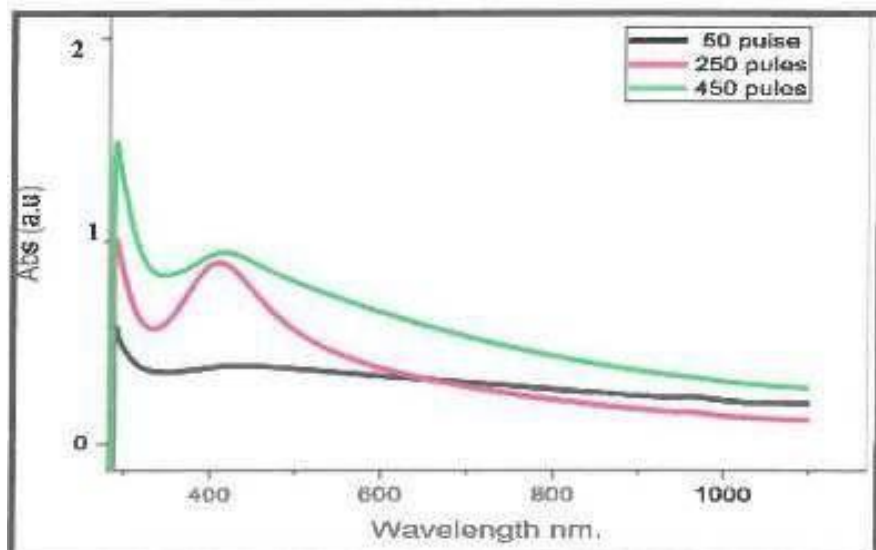


Figure (17) The absorbance for titanium dioxide nanoparticles solution.



**Figure (18) The absorbance of titanium dioxide / silver hybrid nanoparticles solution.**

**Table (2)** presents the findings of surface plasmon resonance (SPR) and the absorption intensity derived from the absorbance spectrum at a wavelength of 1064 nm, energy of 530 mJ, and varying number of pulses.

Nanoparticles in distilled water	Pulses number	Energy (mJ)	Abs(a.u) Absorbency		Peak (nm) (SPR)	
Ag	50	530	0.179		407	
	250	530	0.431		406-409	
	450	530	0.505		410-413	
TiO <sub>2</sub>	50	530	0.525		291	
	250	530	1.021		293	
	450	530	1.708		292	
TiO <sub>2</sub> /Ag	50	530	0.287	291	0.191	413-417
	250	530	0.501	291	0.446	408-413
	450	530	0.738	291	0.472	415-419

## Biological Applications

Various studies have shown that the ability of AgNPs to kill bacteria is greatly affected by their form, size, concentration, and colloidal state. This makes a wide range of nanomaterials a compelling substitute for antibiotics now.

The stability and biocompatibility of AgNPs have been found to be enhanced by size reduction [34]. Hence, it is crucial to engineer nanoparticles with optimal dimensions, morphology, and surface properties to be employed in various clinical and therapeutic applications.

The antibacterial activity of AgNPs increases as their particle size decreases. The antibacterial effect is more noticeable when using smaller nanoparticles. This is intriguing because the attachment of AgNPs to cell membranes and the resulting changes in the lipid bilayer lead to increased membrane permeability, cell harm, and cell death [23,34]. The antibacterial effectiveness of AgNPs is greatly affected by the ratio of surface area to volume and the nature of the crystalline surface. The number 34 is represented as [34].

The inhibition zone test was carried out to qualitatively confirm the antibacterial property of the titanium dioxide and silver nanoparticles and their hybrids prepared with distilled water and with the average size of different diameters obtained with different numbers of pulses (50, 250, and 450) pulses and with an excision card (530 mJ). *Pseudomonas aeruginosa* and were the two kinds of bacteria for which these compounds were employed (*Staphylococcus aureus*).

As the results showed a high inhibitory effect against the two types of bacteria, as shown in Figure (19) and figure (20).

But when the hybrid nanomaterials of silver and titanium dioxide and obtained inhibition in both bacterial classes, the inhibition zone B's appearance of the widest diameter (cm) was obtained.

Only distilled water, a sample without laser ablation, was able to identify the anti-bacterial action (0 mJ). The inhibition was remarkably low compared to samples prepared by laser. Ag, on the other hand, has a long history of being proven to be a powerful antibacterial agent. TiO<sub>2</sub>/ Ag nanocomposite has the performance of extending the antibacterial activity of the nanomaterial to a wider range of operational situation [35].

## Conclusions

This study establishment provides a convenient platform for synthesizing silver and titanium oxide nanoparticles utilizing a nanosecond pulsed laser approach. The produced nanoparticles were tested using X-ray diffraction (XRD), ( FESEM) field emission scanning electron microscopy, (TEM) transmission electron microscopy, also ultraviolet-visible spectroscopy (UV-Vis). The AgNPs submit a color shift from bright green to dark brown, which was confirmed by the UV-Vis spectra that display absorption at a wavelength of 406.3 nm. On the other hand, the TiO<sub>2</sub> NPs appeared white and had an absorption wavelength of 296.4 nm. The peak wavelengths correspond the presence of powerful and synchronized electron oscillations on the surface of the metal. This project provide a potential approaching for the beginning of nanoparticles with highly desired properties for use in antibacterial applications.

## Reference

- 1- NM Jassim, K Wang, X Han, H Long, B Wang, P Lu, Plasmon assisted enhanced second-harmonic generation in single hybrid Au/ZnS nanowires, *Optical materials* 64, 257-261 2017.
- 2- Sabu Th, Saeedeh R., Shima M., Arezo A., Foundations of Nanotechnology, "Nanoelements Formation and interaction", AAP Research notes on nanoscience and nanotechnology, apple academic press.inc, Vol. 2, (2015)..
- 3- TH Mubarak, NM Jassim, QA Guidan, Some physical properties of Al nanoparticle Via pulse laser ablation in liquid method (PLAL), *Academic Science Journal* 1 (2), 66-81 . 2023.
- 4- Official Journal of the European Union. COMMISSION RECOMMENDATION of 18 October 2011 on the Definition of Nanomaterial (Text with EEA Relevance) (2011/696/EU). Available online: [https://ec.europa.eu/research/industrial\\_technologies/pdf/policy/commission-recommendationon-the-definition-of-nanomater-18102011\\_en.pdf](https://ec.europa.eu/research/industrial_technologies/pdf/policy/commission-recommendationon-the-definition-of-nanomater-18102011_en.pdf) (accessed on 11 December 2017) .
- 5- HZ Abdulrahman, ÇY Atao, NM Jassim. PLASMONIC ENHANCEMENT IN MOLECULAR FLUORESCENCE OF NATURAL CURCUMIN DYE WITH SILVER NANOPARTICLES SYNTHESIS & BIOLOGICAL APPLICATION. *Journal of Pharmaceutical Negative Results* 13 (3), 592-603.2022.
- 6- Rusul k. Ismail\*, , Raad M. S. Al-Haddad and Tahseen H. Mubarak ,.Time Effect on the Red Shift of Surface Plasmonic Resonance Core-Shell SiO<sub>2</sub>: Gold Nanoparticles (AuNPs),.Cite as: *AIP Conference Proceedings* 2190, 020095 (2019), Published Online: 11 December 2022.
- 7- M. D. Cheng, D. Lowndes and D. B. Geohegan, "Generation and Characterization Engineered Nanoparticles for Environmental and Billogical Exposure Research, International Symposium on Envirnomental Nanotechnology", Taiwan, pp.1-12, (2004).
- 8- Z. P. Xu, Q. H. Zeng, G. Q. Lu and A. B. Yu, "Inorganic nanoparticles as carriers for efficient cellular delivery", *Chemical Engineering Science*, 61(3), pp.1027-1040, (2021).
- 9- A. R. Siekkinen, J. M. McLellan, J. Chen, and Y. Xia, "Rapid synthesis of small silver nanocubes by mediating polyol reduction with a trace amount of sodium sulfide or sodium hydrosulfide", *Chemical Physics Letters*, 432 (4-6), pp. 491–496, (2006).
- 10- J. Prikulis, F. Svedberg, M. Kall, "Optical spectroscopy of single trapped metal nanoparticles in solution", *Nano Letters* 4 , pp. 115-118, (2004) .
- 11- M. S. Chargot, A. Gruszecka, A. Smolira, J. Cytawa and L. Michalak, "Mass spectrometric investigations of the synthesis of silver nanoparticles via electrolysis", *Vacuum*, 82(10) , pp. 1088–1093, (2008).
- 12- F. G. Rutberg, M. V. Dubina, V. A. Kolikov et al., "Effect of silver oxide nanoparticles on tumor growth in vivo," *Doklady Biochemistry and Biophysics*, vol. 421, no. 1, pp. 191–193, 2008.

- 13- Jenel Marian Patrascu and others Composite Scaffolds Based on Silver Nanoparticles for Biomedical Applications . Hindawi Publishing Corporation Journal of Nanomaterials Volume 2015, Article ID 587989.
- 14- S.-L. Peng, D.-X. Chen, G. Su, Z. Wang, Y. H. Xiao, and Z. L. Liu, "Application of nanometer silver antiseptic dressing for wound surface in children after urinary surgery," Journal of Clinical Rehabilitative Tissue Engineering Research, vol. 11, no. 40, pp. 8181–8183, 2007.
- 15- M. I. Sriram, S. B. M. Kanth, K. Kalishwaralal, and S. Gurunathan, "Antitumor activity of silver nanoparticles in Dalton's lymphoma ascites tumor model," International Journal of Nanomedicine, vol. 5, no. 1, pp. 753–762, 2010.
- 16- M. Rahban, A. Divsalar, A. A. Saboury, and A. Golestani, "Nanotoxicity and spectroscopy studies of silver nanoparticle: calf thymus DNA and K562 as targets," Journal of Physical Chemistry C, vol. 114, no. 13, pp.
- 17- R. Xu, J. Ma, X. Sun et al., "Ag nanoparticles sensitize IR-induced killing of cancer cells," Cell Research, vol. 19, no. 8, pp. 1031–1034, 2009.
- 18- W. Zhang, X. Qiao, and J. Chen, "Synthesis of nanosilver colloidal particles in water/oil microemulsion," Colloids and Surfaces A: Physicochemical and Engineering Aspects, vol. 299, no. 1–3, pp. 22–28, 2007.
- 19- V.-S. Manoiu and A. Aloman, "Obtaining silver nanoparticles by sonochemical methods," UPB Scientific Bulletin, Series B: Chemistry and Materials Science, vol. 72, no. 2, pp. 179–186, 2010.
- 20- O. V. Melnikov, O. Y. Gorbenko, M. N. Markelova et al., "Ag- $\gamma$  doped manganite nanoparticles: new materials for temperaturecontrolled medical hyperthermia," Journal of Biomedical Materials Research, Part A, vol. 91, no. 4, pp. 1048–1055, 2009.
- 21- C.-S. Wu, C.-Y. Lee, J.-K. Chen et al., "Microwave-assisted electroless deposition of silver nanoparticles onto multiwalled carbon nanotubes," International Journal of Electrochemical Science, vol. 7, no. 5, pp. 4133–4142, 2012.
- 22- C. S. Ciobanu, S. L. Iconaru, P. Le Coustumer, L. V. Constantin, and D. Predoi, "Antibacterial activity of silver-doped hydroxyapatite nanoparticles against gram-positive and gram-negative bacteria," Nanoscale Research Letters, vol. 7, article 324, 2012.
- 23- Jassim, N. A. H., Mohamed, A. J. (2021) Experimental implementation of Raman scattering spectroscopy photoluminescence and some optical properties of silver nanoparticles created by eco-friendly technique EUREKA: Physics and Engineering, 6, 00-00. doi: <https://doi.org/10.21303/2461-4262.2021.002147>.
- 24- M. A. Hettiarachchi and P. A. S. R. Wickramarachchi, "Synthesis of chitosan stabilized silver nanoparticles using gamma ray irradiation and characterization," Journal of Science—University of Kelaniya, vol. 6, pp. 65–75, 2011.
- 25- Seul-Yi Lee and Soo-Jin Park "TiO<sub>2</sub> photocatalyst for water treatment applications" Journal of Industrial and Engineering Chemistry, Vol. 19, p.p 1761–1769, 2013.
- 26- Veronika Jašková, Libuše Hochmannová, and Jarmila Vytlasová, " TiO<sub>2</sub> and ZnO Nanoparticles in Photocatalytic and Hygienic Coatings" International Journal of Photoenergy, p.p1-6, 2013.

- 27- Hongbo Shi, Ruth Magaye , Vincent Castranova and Jinshun Zhao, "Titanium dioxide nanoparticles: a review of current toxicological data" *Particle and Fiber Toxicology*, p.p.10-15, 2013.
- 28- Sulistyani "Review of Applications Nanoparticles of TiO<sub>2</sub> and ZnO in Sunscreen" *Proceeding of International Conference On Research, Implementation And Education Of Mathematics and Sciences* ,Yogyakarta State University ,p.p203-212, 2014.
- 29- K. Venkatasubramanian, S. Sundaraj, "Antibacterial activity of Zinc Oxide and Ag Doped Zinc Oxide Nanoparticles against E. coli" , *Chem. Sci. Rev. Lett.*, Vol.3 ,p.p 40-44, 2014.
- 30- K. Gupta, R. P. Singh, A. Pandey, "Photocatalytic antibacterial performance of TiO<sub>2</sub> and Ag-doped TiO<sub>2</sub> against S. aureus, P. aeruginosa and E. coli" ,*Beilstein J. Nanotechnol.*, Vol.4, p.p 345–351, 2013.
- 31- J. Liu, Y. Ge, X. Z. Zhi, "Study of antibacterial effect of polymethyl methacrylate resin base containing Ag-TiO<sub>2</sub> against Streptococcus mutans and Saccharomyces albicans in vitro" , *West China J. Stomatology*, Vol.30 ,p.p 201–205, 2012.
- 32- Faisal Laith Ahmed . Preparation of Nano-TiO<sub>2</sub> and improve its antibacterial activity, Republic of Iraq Ministry of Higher Education and Scientific Research University of Diyala College of Science Department of Physics. 2019.
- 33- ISRAA ALI HAMEED . ,Preparation and study some physical properties of nanoparticles by pulsed laser Ablation in liquids ,University of Diyala /College of Science/ Department of Physics ,2020 .
- 34- M.A.Shaheed, "Synthesis and Application of Nanoparticles Semiconductors," *Msc.thesis*, Babylon University, 2013.
- 35- Ž. Antić,R.M. Krsmanović,M.G. Nikolić, M.Marinović-Cincović, M.Mitrić,S. Polizzi, and M.D.Dramićanin, "Multisite luminescence of rare earth doped TiO<sub>2</sub> anatase nanoparticles, " *Materials Chemistry and Physics*,Vol.135,No.2-3 , pp.1064-1069, 2012.

## تحضير, تشخيص ودراسة الخواص البصرية لثاني اوكسيد التيتانيوم النانوي وخواصها البايولوجية

ندى عبد الهادي كريم

جامعة القادسية /كلية التربية / قسم الفيزياء

### الخلاصة:

تم تحضير دقائق الفضة وثنائي اوكسيد التيتانيوم وهجين الفضة النانوية الخواص التركيبية والبصرية للدقائق النانوية المحضرة في الماء المقطر كوسط نمو باستخدام ليزر النيديميوم- ياك مضبط عامل النوعية بطول موجي 1046 نانومتر وطاقة استئصال قدرها 530 ملي جول. بمعدل تكرار (1) هرتز. تم تشخيص الدقائق النانوية والدقائق النانوية الهجينة باستخدام التحليل الطيفي للشعة فوق البنفسجية المرئية وحيود الشعبة السينية والتحليل الالكتروني الماسح الباعث للمجال وكذلك طاقة تشتت

### الشعبة السينية

تم كشف المجموعات الوظيفية لدقائق الفضة النانوية ودقائق ثاني اوكسيد التيتانيوم النانوية في وسط السائل باستخدام تقنية تحليل فورير للشعبة تحت الحمراء تظهر الدقائق الكروية النانوية والدقائق المايكروية في مجهر الالكتروني النافذ الذي استخدم في التشخيصات البصرية. الطول الموجية (284.1) و (418.3) نانومتر توافق اطراف المتصاص لمحلول يحوي على دقائق الفضة النانوية. ان دقائق الفضة و دقائق ثاني اوكسيد التيتانيوم النانوية وهجين النانوي المحضر بنسبة

$AgTiO_2$  (1:1, 1:2). تم تشخيصها واستخدامها للتطبيقات البايولوجية.

اظهر طيف الشعبة فوق البنفسجية والمرئية لدقائق الفضة النانوية النقية ذروة امتصاص واسعة قليل في النطاق ( 1:3) (384-410 نانومتر وهو ما يميز رنين البلازمون النانوي من فاتح الى غامق عند زيادة عدد نبضات الليزر. وهذا دليل على تكوين محلول يحتوي على دقائق معدنية نانوية في الماء المقطر اظهرت المواد النانوية المحضرة نشاطا واعداد ضد مسببات

المراس البكتيرية مثل بكتريا القولون والمكورات العنقودية الذهبية.

كلمات مفتاحية: الفضة وثنائي اوكسيد التيتانيوم الهجين, الاستئصال بالليزر, المواد النانوية الهجينة, التطبيقات البايولوجية.